Temporal Variation of Road Dust Load and Its Size Distribution—a Comparative Study of a Porous and a Dense Pavement

Joacim Lundberg · **Mats Gustafsson** · **Sara Janhäll** · **Olle Eriksson** · **Göran Blomqvist** · **Sigurdur Erlingsson**

Abstract Resuspension of road dust contributes to air quality issues with resulting health impacts. Limited studies imply that porous pavements can initially mitigate PM_{10} emissions by acting as a dust trap, but the abrasion wear generates road dust and thus accelerates the clogging processes. In addition, knowledge regarding the impact of pavement types on road dust load dynamics is limited. Road traffic noise can be mitigated using porous pavements, but the use of studded tyres increases the abrasion wear of the pavement as well as increasing the noise emission. Due to this durability problem, porous pavements are rarely used in the Nordic countries where, instead, dense pavements which are abrasion resistant are more common. Linköping municipality, in Sweden, constructed a porous pavement to mitigate road traffic noise. This led to the opportunity to investigate the temporal variation of the dust load dynamics and inherent size distributions over the winter and spring in comparison to those of an adjacent dense pavement. Results, when using the wet dust sampler (WDS) method, showed similar dust load dynamics for the dense and porous pavements. The results were also compared to previous studies using the same method on different dense pavements in Stockholm, Sweden. All locations showed a seasonal variation with higher dust loads during winter and early spring and declining loads towards summer. The size distributions were more complex for the wheel tracks at the porous pavement, having primarily properties of a mixture model compared to the simple size distributions for the dense pavement. On the other hand, the dust load and size distribution were more similar between the porous and dense pavements regarding loads and shapes, indicating a less pronounced but similar behaviour between the surfaces outside of the wheel tracks.

Keywords Road dust · Organic fraction · Particle size distribution · Temporal variation · Stone mastic asphalt–SMA · Double-layered porous asphalt concrete–DLPAC · Low noise pavement

J. Lundberg (✉) · M. Gustafsson · O. Eriksson · G. Blomqvist · S. Erlingsson
Swedish National Road and Transport Research Institute – VTI, 581 95 Linköping, Sweden
e-mail: joacim.lundberg@tft.lth.se

J. Lundberg · S. Erlingsson
Division of Building Materials, Royal Institute of Technology – KTH, Stockholm, Sweden

S. Janhäll
Research Institutes of Sweden – RISE, Borås, Sweden

S. Erlingsson
Faculty of Civil and Environmental Engineering, University of Iceland, Reykjavik, Iceland

1 Introduction

Particle air pollution has been on the agenda since the 1950s, with an ever-increasing focus on the health impacts on humans (WHO 2005; WHO 2016) and the resulting socioeconomic impact (e.g. WHO Regional Office for Europe OECD 2015). Health impacts include, but are not limited to, cardiovascular and cerebrovascular

mortality, respiratory diseases and daily mortality (e.g. Brunekreef and Forsberg 2005; Forsberg et al. 2005; WHO 2005; Meister et al. 2012; Stafoggia et al. 2013).

Generally, anthropogenic sources are the most important in urban environments, where larger populations are exposed. Particle sources include industries, construction sites (e.g. Kampa and Castanas 2008), residential heating (e.g. biomass burning) (e.g. Sigsgaard et al. 2015) and traffic sources, which in turn can be further divided into exhaust emissions (e.g. Burtscher 2005) and direct non-exhaust emissions from road, tyre and brake abrasion wear (Gustafsson et al. 2008; Thorpe and Harrison 2008; Gustafsson et al. 2009; Harrison et al. 2012; Grigoratos and Martini 2015), as well as suspension/resuspension of road dust (China and James 2012; Amato et al. 2014a; Amato et al. 2016; Padoan et al. 2018; Stojiljkovic et al. 2019). Exhaust particles are regulated with increasing restrictions, while non-exhaust sources are unregulated, despite having greater health impact than previously thought (WHO 2013; van der Gon et al. 2013; Amato et al. 2014b).

For northern countries, direct and resuspended non-exhaust sources dominate the PM_{10} (particulate mass with and aerodynamic diameter < 10 μm) composition (WHO 2005; Gustafsson et al. 2011). With current development in technology and regulations, exhaust sources decrease, thus increasing the relative abundance of non-exhaust particles (e.g. Timmers and Achten 2016). Especially countries using studded tyres have problems with anthropogenic mineral dust due to increased pavement wear (Denby et al. 2013; Norman et al. 2016; Lundberg et al. 2019b) increasing direct particle generation and dust load (Gustafsson et al. 2008; Hussein et al. 2008; Kupiainen and Pirjola 2011). This also applies to traction sanding since the sand, especially in combination with studded tyres, both accelerates the abrasion wear of pavements and in itself is crushed into finer dust (Kupiainen 2007; Kupiainen and Pirjola 2011; Kupiainen et al. 2016). The increased abrasion wear from studded tyres has led to an increased use of abrasion wear resistant pavements, such as the stone mastic asphalt (SMA). This dust load is stored on road surfaces and contributes to particle concentrations in air due to suspension from traffic and wind. The dust contains particles directly contributing to PM_{10} as well as larger particles, which have the potential to be further crushed/fragmented and contribute to PM_{10} emissions.

There are several transport mechanisms impacting on dust load dynamics, and in extension PM_{10} concentrations, including mass transport to the surface (e.g. through deposition), accumulation of dust on the surface (e.g. wetness binding dust to the surface) and transport away from the surface (e.g. wind shear suspending particles). These processes depend on the road surface texture but are also influenced by the surface wetness, and meteorological conditions, including wind, dew and precipitation. Also, wintery road surface conditions like ice and snow cover strongly affect the generation and transport of road dust. The tyres' interaction with the road surface also impacts on the transport of particles. Wet conditions suppress suspension of particles. Dust instead accumulates in the macrotexture of the surface. Given sufficient amounts, flowing water can transport dust to or away from the surface, depending on road construction properties such as crossfall. Splash and spray from road surface and tyre interaction can transport dust to or from the surface, with both mechanisms affected by the macrotexture of the surface (PIARC 1987). For icy and snowy conditions, dust can also be removed/introduced by removal, or melting, of snow. During dry conditions, dust is primarily suspended due to tyre interaction and wind shear from both natural wind and moving traffic. Direct emissions of non-exhaust particles are also higher during dry conditions. The highest suspension forces are applied to the wheel tracks through both direct tyre interaction with the surface and turbulent air flow around the vehicle. Tyres rolling over a surface will entrap and compress air in the cavities of the road surface macrotexture. When the air is released, suspension occurs due to wind shear. This mechanism, called "air-pumping" has already been studied regarding the noise that is generated when the air is released (e.g. Eisenblaetter et al. 2010). Due to the high suspension forces, the road dust load is seldom high in wheel tracks, and the actual suspension from individual vehicles is low. Between wheel tracks suspension forces are lower, and suspension occurs only due to the turbulent air flow from the moving vehicle, thus reducing the transport effect. Towards the edge, wind shear due to turbulent air flow from vehicles still occurs, diminishing with distance from the traffic, making the suspension even less effective. Surfaces outside the wheel track have normally higher dust loads due to lower suspension forces, but if a vehicle happens to drive out of wheel tracks, the momentary suspension from these surfaces will be high. The tyre will also

directly transport particles during dry and wet conditions where particles get stuck to the tyre tread. These vehicles induced dust transport processes depend on both traffic characteristics (speed and composition), meteorological conditions (especially precipitation and surface moisture), road design (such as cross fall and macrotexture) and road conditions such as cracks and rutting.

Little is known about how pavement types and conditions affect the temporal variation of road dust load dynamics. Most of the studies available have been performed in the Nordic countries, focusing on dense pavement, primarily different types of SMA. The most extensive study is presented in Gustafsson et al. (2019b) where the mineral dust loads, expressed as DL_{180} in Stockholm, Sweden, were studied for 6 years. The study showed a clear seasonal pattern for all investigated streets with lower dust loads in, rather than between, wheel tracks. During summer and early autumn, dust loads are low. During late autumn and winter, dominated by wet, snowy and icy road surface conditions, dust load accumulates. Furthermore, mineral dust generation is accelerated by both the use of studded tyres, which increases the abrasion wear of pavements, and by the use of traction sanding. Throughout spring, when conditions change from wet to dry, dust loads decrease due to the increased suspension, causing high PM_{10} concentrations, with a clear impact on air quality. During spring, studded tyres are also exchanged for summer tyres, decreasing the generation of mineral dust. Dust loads decrease further during summer, and the cycle is then repeated. The study also showed that replacing an old SMA with a new, more abrasion wear-resistant SMA with a rougher initial macrotexture, the dust load was increased during the first winter. While the dust load increased, air quality (PM_{10}) was, however, initially improved, although likely affected by the changes in the traffic situation (Elmgren 2018).

There are more environmental aspects than air quality that can influence pavement choice. Road traffic also generates noise from the road surface and tyre interaction (e.g. Sandberg and Ejsmont 2002; Vieira 2018). Noise, as air pollution, can cause health problems including cardiovascular diseases, annoyance, sleep disruption and cognitive impairment in children (e.g. WHO 2011). For roads with traffic speeds above about 40–50 km/h, the noise from the road surface and tyre interaction dominates (Sandberg and Ejsmont 2002; Vieira 2018). To reduce noise generation from tyre interaction with the road surface, dense pavements can be replaced by porous pavements, such as double-layered porous asphalt concrete (DLPAC). The interconnected air voids in the DLPAC reduce some of the noise generation mechanisms (Sandberg and Ejsmont 2002; Vieira 2018), and these voids may also affect abrasion wear and resuspension of dust and thus the particle concentrations in the air. The lower durability of the porous pavements compared to SMAs causes DLPACs to be uncommon in the Nordic countries where the usage of studded tyres increases abrasion wear and ravelling, i.e. loss of aggregates due to failure in the binding holding aggregates together. Abrasion wear and road dust also increase air void clogging rates, thus decreasing the acoustical lifespan, i.e. the time until significant noise reductions are no longer obtained. Since DLPACs are more complicated to construct and maintain and have lower durability against abrasion wear and ravelling, making studded tyres cause lower life span and increased cost, it is mainly attractive when noise reduction from road traffic is essential. The most successful example in Sweden gave an initial noise reduction of 7–8 dB(A) with an acoustical lifespan of about 7 years, compared to the expected 3 years (Sandberg et al. 2018; Vieira et al. 2019). DLPACs have not been investigated regarding dust loads and only briefly examined regarding potential impact on air quality (Gustafsson and Johansson 2012; Norman and Johansson 2017; Elmgren and Norman 2019; Vieira et al. 2019; Lundberg et al. 2019c). The air quality studies available present initial positive results with lower particle emissions compared to a dense reference pavement, with a diminishing effect after 3 years of service (Norman and Johansson 2017; Elmgren and Norman 2019). This suggests that the DLPAC act as a particle trap. Had the particle emissions been primarily due to abrasion, the effect would be more constant rather than diminishing over time. However, it is still unknown how the porous pavements' internal structure impact on both dust load and, in extension, on air quality as seen for dense pavements.

Due to problems with road traffic noise, Linköping municipality decided to replace an old SMA with a DLPAC on a part of the street Industrigatan within Linköping City in order to mitigate the tyre/road traffic noise. This change of asphalt was used to compare the development of dust load and the particle air concentrations close to the DLPAC (not presented in this paper) while the adjacent remaining SMA pavement was used

as a reference. Part of these investigations is presented in this paper with the aim to investigate the following:

- How a porous pavement impact on the temporal variation of road dust load compared to a dense pavement.
- How a porous pavement impact on the temporal variation and shape of road dust load size distribution compared to a dense pavement.

2 Methods

2.1 Site Description

The investigated SMA and DLPAC pavements are located at Industrigatan in the city of Linköping, Sweden, with their location and the sampling locations as shown in Fig. 1. All measurements were performed in the northbound driving lane as this direction had only one lane, giving exactly the same amount of traffic passing both sites. In the southbound direction, the number of lanes changed between the sites. The sites are rather similar, though the SMA site has a more open street canyon with woodland on the west side and uncultivated grassland on the east side and a noise barrier in direct connection to the road. The DLPAC site has a more closed street canyon, where the west side has woodland in direct connection to the road as at the SMA site, while the east side has a stretch cultivated grass lawn and woodland in direct connection with the road.

2.2 Pavement Information

The DLPAC was constructed during early August 2018. To investigate the pavement construction, drill cores were collected for both the SMA and the DLPAC. Six drill cores were collected for the DLPAC at two locations in the northbound lane, with one core taken in the left wheel track, between wheel tracks and in the right wheel track, respectively. The cores were collected early in November 2018, about 2 months after construction, before any impact of studded tyres or deformation could occur. For the SMA, three drill cores were collected during January 2019 close to the edge in the southbound lane. Engineering judgement and visual inspection gave an estimated pavement age of 6–10 years for the SMA.

Due to unrepresentative grain size distribution and the visual inspection at the site, one SMA drill core was disregarded. Both the design values and the drill core analyses are presented in Table 1. Due to the lack of design information for the SMA, the Swedish Transport Administration's limited values for SMA (Swedish Transport Administration 2011) were used as proxy values for typical design. As seen in Table 1, the DLPAC deviated from the design values, especially for the bottom layer, while the SMA was close to the proxy limit values, showing the importance of using drill cores and not only trusting theoretical information. A tomography scan of one of the DLPAC drill cores is given in Fig. 2, showing the difference in air voids between the layers.

2.3 Traffic Situation

Industrigatan has an annual average daily traffic (AADT) of 14,700 vehicles, with the proportion of heavy traffic being 7%. The speed limit is 70 km/h. The lateral distribution of vehicles was measured using a traffic camera system from Viscando AB. The measurement location was at the DLPAC (see Fig. 1). The camera has a time resolution less than 1 s and registers all passing vehicles' speed, lateral position and vehicle class (either light or heavy). The lateral position is based on the system's estimate of each vehicle's centre of gravity. The lateral distribution of vehicles is presented in Fig. 3. The position was recalculated from the vehicles' centre of gravity to the lateral position of the two tyres. The calculation was performed using the three vehicle groups described in McGarvey (2016), where light vehicles had an approximate axle width of 1.5 m, and the two heavy goods vehicle classes had approximate axle widths of 1.8 and 2.1 m, respectively, and was here set to the mean value 1.95 m. The lateral distribution was not known during the road dust samplings using the Wet Dust Sampler (WDS, further described below). Instead, visual inspection determined the sampling location of right and left wheel tracks. The WDS sampling locations were shifted compared to the actual position of the traffic (Fig. 3) due to less pronounced wheel tracks during the first winter season, since the surface course had not sustained much abrasion wear.

The proportion of light vehicles using studded tyres was measured on nine occasions, since heavy vehicles do not use studded tyres in Sweden. For each measurement, the first 200 light vehicles were counted, and the use of
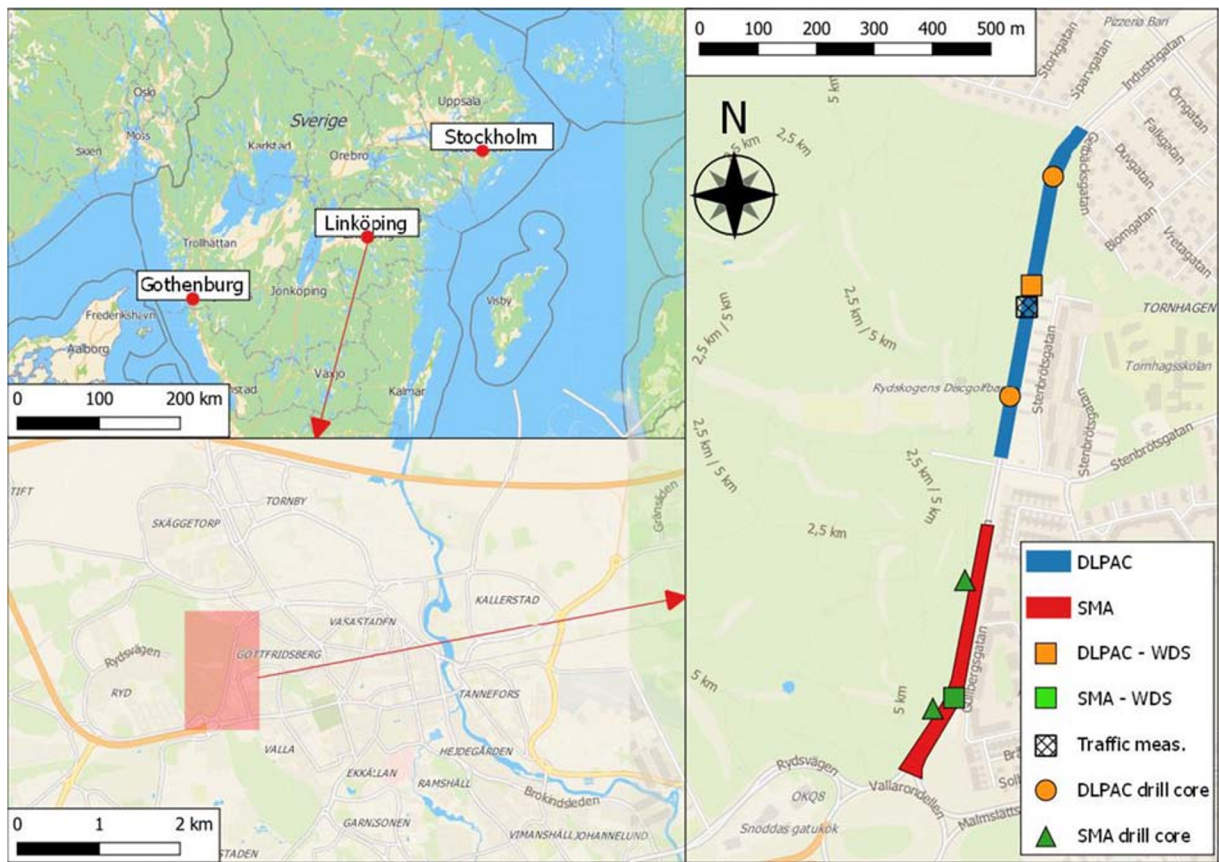
Fig. 1 Map showing part of southern Sweden, the location of Linköping and the location of Industrigatan. DLPAC, double-layered porous asphalt concrete; SMA, stone mastic asphalt; WDS, wet dust sampler sampling locations. All markings are approximate. Map is modified from © OpenStreetMap contributors, CC-BY-SA

studded tyres was determined by two operators by listening, since studded tyres generate a distinct sound. If one operator was uncertain and the other operator marked the vehicle as having studded tyres, it was more likely that the vehicle had studded tyres than not. For one occasion, an estimate of potential mislabelling was performed by determining the number of times either operator became uncertain. The proportion of studded tyres determined by

Table 1 Pavement information for the DLPAC and SMA pavements. The design values are presented together with drill core analysis values. All spans represent the minimum and maximum values. The letter n denotes number of drill cores used for the analysis. Note that for DLPAC, the same drill cores were used, with the top and bottom layer separated prior to the analyses

Pavement type	Layer	Maximum aggregate size (mm)		Void content (%)		Layer thickness (mm)		Binder content (%)		Pavement age	n
		Design value	Drill core analysis	Design value	Drill core analysis[ii]	Design value	Drill core analysis[iii]	Design value	Drill core analysis[iv]		
DLPAC	Top	11	11	23.1	18.6–23.4	25	20–30	6.6	6.0–6.3	1–2 months	6
	Bottom	16	16	23.1	6.1–10.8	55	35–60	6.4	6.4–6.8	1–2 months	6
SMA	–	16[i]	16	2.0–3.5[1]	< 3.5	–	–	5.8–6.0[i]	6.1–6.3	6–10 years[v]	2

[i] Based on the Swedish Transport Administration limit values as proxy since Industrigatan is a municipal road and not part of the state network. Source: Swedish Transport Administration (2011). [ii] Determined by CEN (2018). [iii] Measured using the drill cores. [iv] Determined by CEN (2012). [v] Estimated
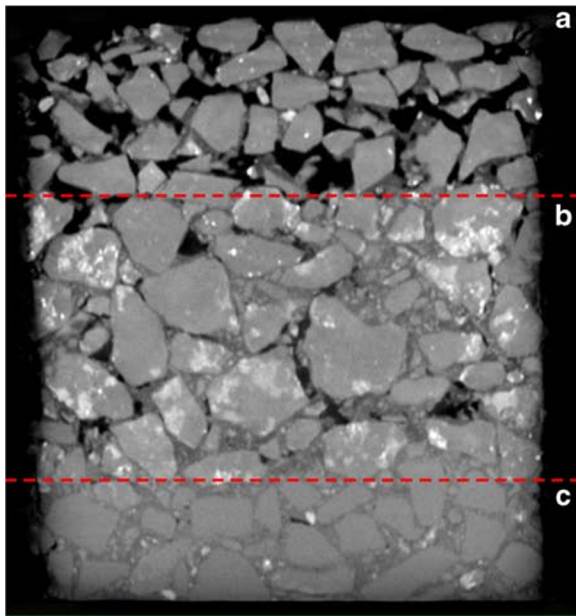
Fig. 2 Digital X-ray computer tomography scan of one of the DLPAC drill cores. **a** The top layer of the DLPAC. **b** The bottom layer of the DLPAC. **c** An old dense pavement. Note the interconnected voids in the top layer (**a**), and the lack thereof in the bottom layer (**b**). The black areas are the air voids, while grey and white areas are asphalt mastic (binder and filler) or mineral aggregates

listening was compared to measurements done at a large parking space outside the IKANO building in the commercial district of Tornby, Linköping. The proportions of studded tyres are presented in Fig. 4, showing similar results.

2.4 Methods for Road Dust Sampling and Characterisation

There are different ways to sample road dust, mainly divided into wet methods like cleaning the surface with water as compared to dry methods like using suction, brushing or wind shear to move the particles from the surface to the sample (Amato et al. 2009; Etyemezian et al. 2007; Lundberg et al. 2019a). In Sweden, the road surface is wet (or even snowy) during most of the winter season and the dry methods would not be useable as the wetness of the surface, and not the amount of dust on the road, is the main factor in determining the amount of dust collected. Not even a wet method can be used during times with snow cover or during very low temperatures (as the sampling water might freeze).

2.4.1 Wet Dust Sampler

Road dust was sampled using the own-developed Wet Dust Sampler (WDS) at both sites (Jonsson et al. 2008; Lundberg et al. 2019a). The sampling device is placed on the sampling surface, and a small circular area is sealed by the operator standing on the foot plate, pressing a cellular rubber ring into the road surface texture. The sample is then taken by an automated procedure during which the surface is washed with a known volume of water (about 350 g) at high pressure for a set amount of time. Thereafter, the dust laden water is transferred into a container using filtered compressed air. One such procedure will be referred to as a "shot" in the text. Settings used were water delivery stops after 5 s, sample transfer starts after 2 s and the full shot ending at 10 s, as used in previous studies (Gustafsson et al. 2019b; Lundberg et al. 2019a). Deionized water was used.

2.4.2 Field Sampling

The sampling at Industrigatan was carried out using a similar strategy as in Gustafsson et al. (2019b), where six shots were taken in one container to form one sample. At the SMA site, three samples were taken for each category: left wheel track (LW), between wheel tracks (BW), right wheel tracks (RW) and the edge (E), giving 12 samples per test. At the DLPAC site, the number of shots per sample varied both during and between sampling tests since the pavement was designed to drain water from the surface. The sampling continued until a visual comparison showed that the DLPAC container had a similar amount of water as the SMA container. The number of shots per sample was registered for the analysis of the data. A general description of the sampling strategy, the categories and the amount and distances between shots are shown in Fig. 5. The placement of left, right and between wheel tracks was visually determined at the first sampling occurrence. Traffic measurement data (Fig. 3) later showed that the sampling positions were slightly shifted compared to the actual position of the traffic. Both sites were marked to ensure that all subsequent measurements were taken within the same areas. Before and after each sampling test, the delivered mass of water from the WDS was controlled by flushing directly into a pre-weighed container. A total of three to six delivered water masses were recorded, with the average used in
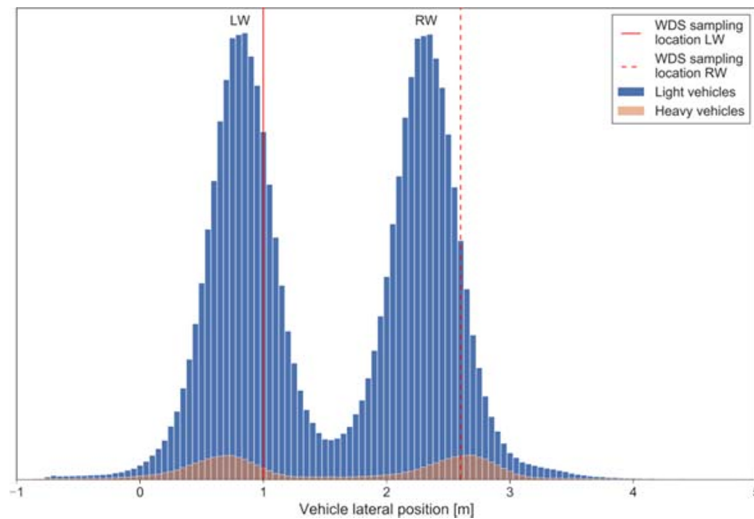
Fig. 3 Histogram of the lateral distribution measured between 2019-01-09 and 2019-04-16 for the northbound lane. Number of bins was 120, i.e. each bin corresponding to 5 cm. Lateral position 0 m corresponds to the approximate left edge of the northbound driving lane. Negative values correspond to the tyre being in the second southbound lane. No vertical scale is given since the interest is the lateral position and the WDS sampling location rather than the exact numbers of passing vehicles. LW and RW mark left and right wheel track, respectively

the calculation steps described later. To avoid potential biological growth, all containers were stored at about + 4–5 °C in darkness until processed in the laboratory, commonly about 1 to 4 weeks. Sampling was performed at night, and to mark the sampling occasion, the date of the following morning was used.

2.4.3 Laboratory Processing of WDS Samples

The following steps were used, and have been used for all earlier published data of DL_{180}, for each sample

when determining all parameters (masses) required to calculate the DL_{180} (mineral dust load < 80 μm):

1. The containers with samples are weighed.
2. All samples are sieved separately through a 180-μm sieve to remove the largest particles, primarily to remove sand and grit since one grain can heavily influence the resulting particle masses and calculations. The sieving also makes the DL_{180} backwards comparable to earlier WDS studies (e.g. Gustafsson et al. 2019b). Additionally, the size is close to the
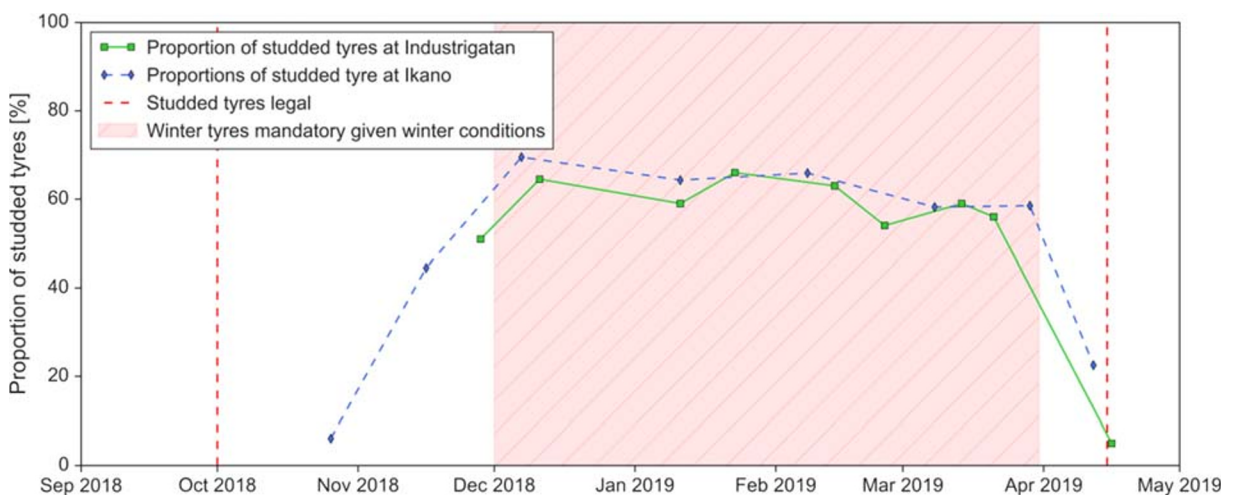

Fig. 4 The proportions of studded tyres in Linköping at Industrigatan and at the IKANO parking space in Linköping. For Industrigatan, the lower uncertainty was 6.5%

upper limit of 200 μm used for dust loads in the NORTRIP (non-exhaust road traffic induced particle) emission model (Denby et al. 2013).

- If size distribution is to be determined, a subsample of approximately 200 ml is taken from the sieved dust-laden water. The sample is stored at + 4–5 °C in darkness until analysis, commonly 1 to 4 weeks, to avoid biological growth. The material left continues to step 3. The mass dust-laden water removed is accounted for later in the calculations.

3. The sieved sample is filtered using vacuum filtering. The pressure is set to 10 mbar. A Büchner funnel is used in which a pre-weighed Munktell 00H filter with a diameter of 125 mm has been placed.

- If the filter becomes saturated, the dust laden water is transferred back to its container, and the first filter is replaced by a second pre-weighed filter, etc.

4. After filtration, the filter(s) are covered and dried in a heater at 60 °C for at least 8 h (overnight).

- If particles are left in the funnel after filter removal, part of a pre-weighed filter is used to collect them and then placed with the other filter(s).

5. After drying, the filter(s) are cooled to room temperature and weighed.
6. The samples are burned at 550 °C for a minimum of 6 h in pre-weighed crucibles with lids.
7. After burning, the crucibles are cooled to room temperature and weighed on an analytical balance.

The analytical balance has only been used when indicated, and had a precision of 0.1 mg, while all other weights were recorded using a balance with a precision of 100 mg.

For each sampling occurrence, the second sample collected in each category (left wheel track, between wheel tracks, right wheel track and edge) were selected to perform the size distribution analysis, as described later.

2.4.4 Calculation of DL_{180}

Using the masses of water and particles from the laboratory steps, the DL_{180} is calculated. The first step calculates the corrected water mass $M_{w, corr}$ (g):

$$M_{w,\text{corr}} = M_{w,\text{sample}} - M_{p180,\text{sample}} \tag{1}$$

where $M_{w, sample}$ is the mass of the dust-laden water after sieving (g) and $M_{p180, sample}$ is the mass of particles < 180 μm in the sample (g). The mass of particles after burning is used to calculate the mineral dust load. The second step corrects the mass of particles $M_{p180, corr}$ (g):

$$M_{p180,\text{corr}} = M_{p180,\text{sample}} \bullet \frac{M_{w,\text{WDS}} \bullet n_{\text{shots}}}{M_{w,\text{corr}}} \tag{2}$$

where $M_{w, WDS}$ is the average mass of delivered water during WDS sampling (g) and n_{shots} is the number of shots the sample container held (−). Finally, the DL_{180} (g/m²) is calculated as

$$DL_{180} = \frac{M_{p180,corr}}{A_{\text{WDS}} \bullet n_{\text{shots}}} \tag{3}$$

where A_{WDS} is the sample surface area of the WDS (0.002043) (m²). Since the mass of mineral particles was used, comparisons can be made to Gustafsson et al. (2019b). To calculate $DL_{180,tot}$ instead, thus including both mineral and organic material, the mass particles after burning replace the mass before burning.

The calculations are based on the assumption, for dense pavements, that the particle concentration is equal in the collected sample and the water potentially retained on the sampling surface, see Lundberg et al. (2019a) for more information. These calculations adjust the dust load by considering the water, and thus particles, lost during sampling. This assumption is also used for the porous pavement.

2.4.5 Determination of Size Distributions

The size distributions were determined by using laser granulometry (Mastersizer 3000 from Malvern Panalytical using laser diffraction). A laser beam was passed through the (dispersed) sample with particles, causing light scattering. The scattering pattern was analysed by a commercial software calculating the particle size distribution using the Mie scattering model. The refraction index used was based on earlier

Fig. 5 Site description and example on WDS sampling at **a** the northern site with the DLPAC and **b** the southern site with the SMA. Arrows indicate the traffic direction; the white circles are an example of WDS sampling, and the green areas mark the ditches. The distance between the white circles was, in general, about 1–2 dm for all shots along the road. The number of white circles varied but is here kept the same for clarity. LW, left wheel track; BW, between wheel tracks; RW, right wheel track; E, edge
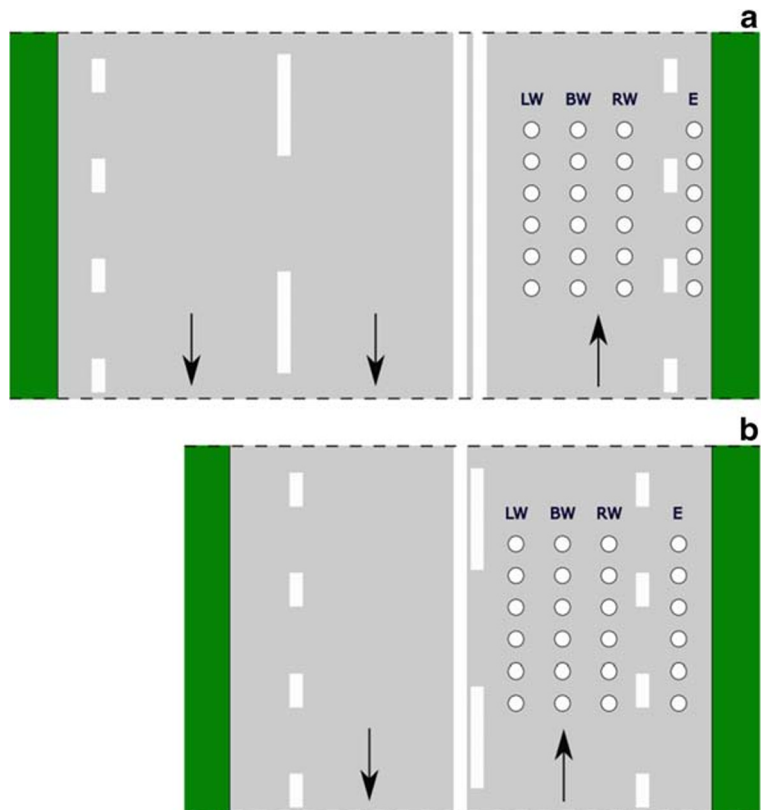
measurement experiences from e.g. Gustafsson et al. (2019b) and engineering judgement. The Mastersizer consists of the main optical unit which transmits red and blue light, a wet dispersion unit (Hydro EV) and a measurement cell which measures the scattered light intensity. Each laser granulometry measurement is carried out by taking three measurements and then calculating the average. The measured size distribution is presented as a volume density. All road dust samples were measured using the following methodology:

1. An initial measurement is performed.
2. Dispersion of sample for 60 s at 1700 rpm.
3. Measurements of the dispersed samples are performed until the measurements stabilises. The measurement with least spread and the lowest weighted residual < 1% is accepted.

Absolute size distributions are calculated by multiplying the $DL_{180,tot}$ with the corresponding volume density (the volume of particles within a size bin described as %). The $DL_{180,tot}$ was used instead of DL_{180} since the size distribution analysis sample was collected

before burning and thus contained both mineral and organic particles.

3 Results and Discussion

3.1 Variation Between Pavement Types and Temporal Variation of Road Dust Load

The mineral dust loads in the left wheel track and between wheel tracks is presented in Fig. 6. Similar WDS samplings of seven different dense pavements performed in central Stockholm, Sweden, by Gustafsson et al. (2019b) are included in the figure for comparison. A clear seasonal variation of mineral dust loads was seen in Linköping for both pavements, similar to the seasonal variation seen in Stockholm. The dust load between wheel tracks was higher in Linköping, with the exception of December for the SMA. In the left wheel track instead, the dust loads were generally lower in Linköping, probably related to a higher speed (70 km/h) and suspension than on the Stockholm streets (30–50 km/h).
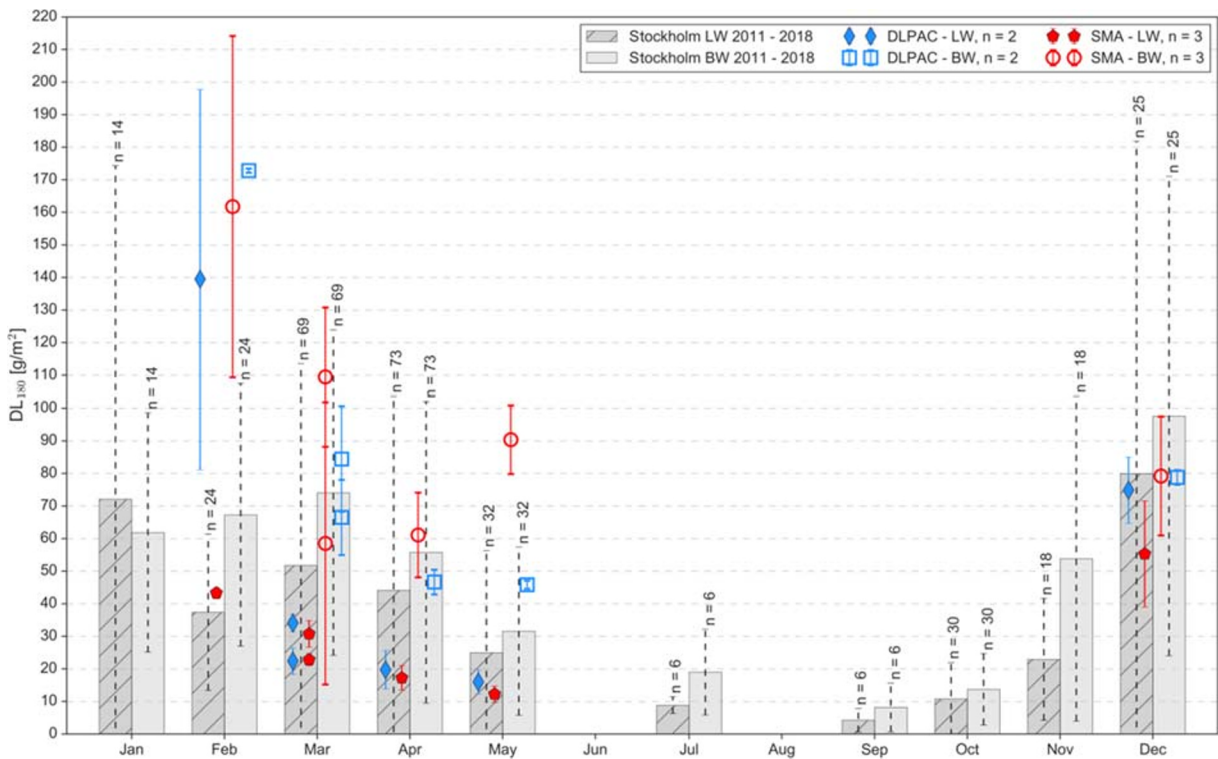
Fig. 6 A comparison between the DLPAC and SMA at Industrigatan, Linköping. The bars express the average DL_{180} and the error bars express the standard deviation. The measurements from Industrigatan shown are the mean value and standard deviation for measurements in that month. The letter n marks number of observations. LW, left wheel track; BW, between wheel tracks. In February, two measurements took place at DLPAC and SMA at Industrigatan. Available measurement data from Stockholm (Gustafsson et al. 2019b) has been is added to the Figure for comparison

For the DLAPC, similar results can be seen for both the wheel track and between wheel tracks measurements. A significant difference between the cities was the use of dust binding and frequent street cleaning, using, amongst others, vacuum technology in Stockholm. It is possible that the dust binding, exposed to tyres, reduces the cleaning efficiency in the wheel tracks, causing less efficient removal of dust in the macrotexture and adding a possible explanation as to why Linköping had generally lower dust loads in wheel tracks. Between wheel tracks, the non-cleaned Linköping street generally had higher loads than in Stockholm, where the dust load between wheel tracks was reduced by street cleaning and where dust binding was used but was not exposed to tyres.

The temporal variation of DL_{180} in Linköping for the SMA and DLPAC is presented in Fig. 7. The mineral dust levels were, in general, higher during winter compared to late spring for all categories. The lateral distribution of dust showed, in general, highest dust loads at the edge, lower dust loads between wheel tracks and lowest dust loads in the two wheel tracks for the SMA.

The dust load on the DLPAC showed, in general, a similar behaviour as for the SMA for the different categories (i.e. in wheel track or between wheel tracks), although with no clear difference, with the exception of the edge where the dust load was lower for the DLPAC. The left wheel track 2019-02-08 was different and showed similarity to the measurements for between wheel tracks and the edge, making it plausible that these samples were taken outside of the wheel track. The design of the DLPAC, with high void content, altered how the tyre interacted with the surface compared to dense pavements. The high void content decreased the surface available for the tyre to interact with and could thus possibly have decreased the abrasion wear of the pavements. The problems with ravelling will still be present. The interconnected voids also affected the storage capabilities. Instead of only storing the dust on top of the surface in the road surface macrotexture (e.g. Lundberg et al. 2017), as for dense pavements such as
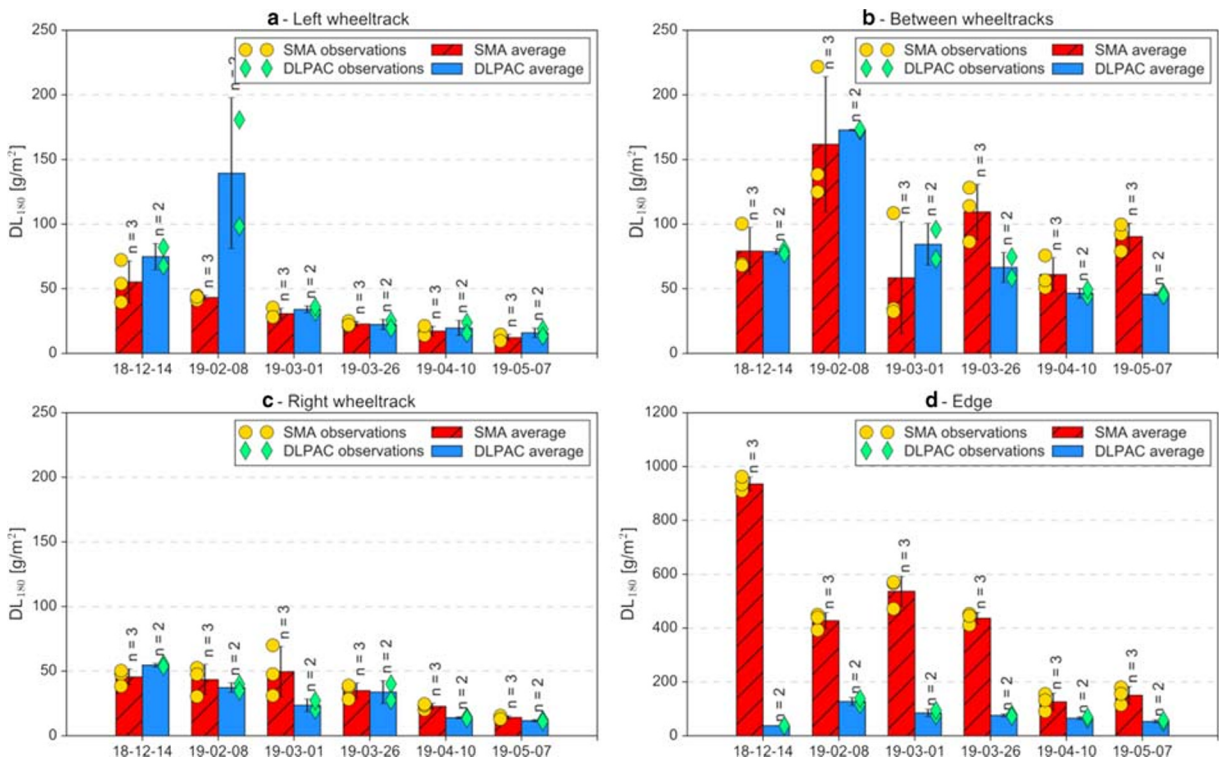
Fig. 7 The variation of DL_{180} for the categories left wheel track (**a**), between wheel tracks (**b**), right wheel track (**c**) and the edge (**d**) for the DLPAC and the SMA. The error bars express the standard deviation. The letter n marks number of observations. Note the different scale on the y-axis in **d**

the SMA, the dust can be transported into the voids which will act as a particle trap. This process was also suggested by the few air quality studies (PM_{10}) available. The interconnected voids will also transport air into the pavement, likely making dust suspension less effective than on dense pavements, since the "air-pumping" effect will decrease, as well as affecting other aerodynamic processes. Wet transport processes, both runoff, splash and spray were also reduced since the water, with dust, was drained into the pavement rather than stored on the surface. Over time, both the dry and wet processes will cause clogging, i.e. reducing the interconnected voids and thus reduce the efficiency of the particle trap, and the DLPAC will thereafter approach the behaviour of dense pavements. When the DLPAC is clogged, particles are no longer transported into the pavement and are instead available again for suspension.

There is always a slight difference between sites in a real situation, even if, as in this case, the sites are similar and placed directly after one another on the same street. Still, the SMA site had a minor curvature (left curve in

northbound lane) with a somewhat wider lane compared to the DLPAC. Previous studies have established that the lateral wander of traffic increases with increasing lane width (e.g. Erlingsson et al. 2012; McGarvey 2016; Lundberg et al. 2019b). The channelling of the traffic in a curve, as on the DLPAC site, will always be slightly different from the straight road, and thus it is possible that the right wheel track might be slightly less pronounced, as compared to the left wheel track, as can be seen in Fig. 3.

The construction of the DLPAC also impacts the results. The top layer reasonably conformed with the intended design based on the drill core analysis, while the bottom layer had a lower air void content than the intended design (Table 1). Since the top layer was only 20–30 mm deep, a bottom layer fulfilling the design could be speculated to transport dust away more efficiently, making the dust less accessible. This implies that the reported dust loads can be considered maximum values, given the circumstances. Samplings were carried out only during the first year in service. Due to clogging over time,
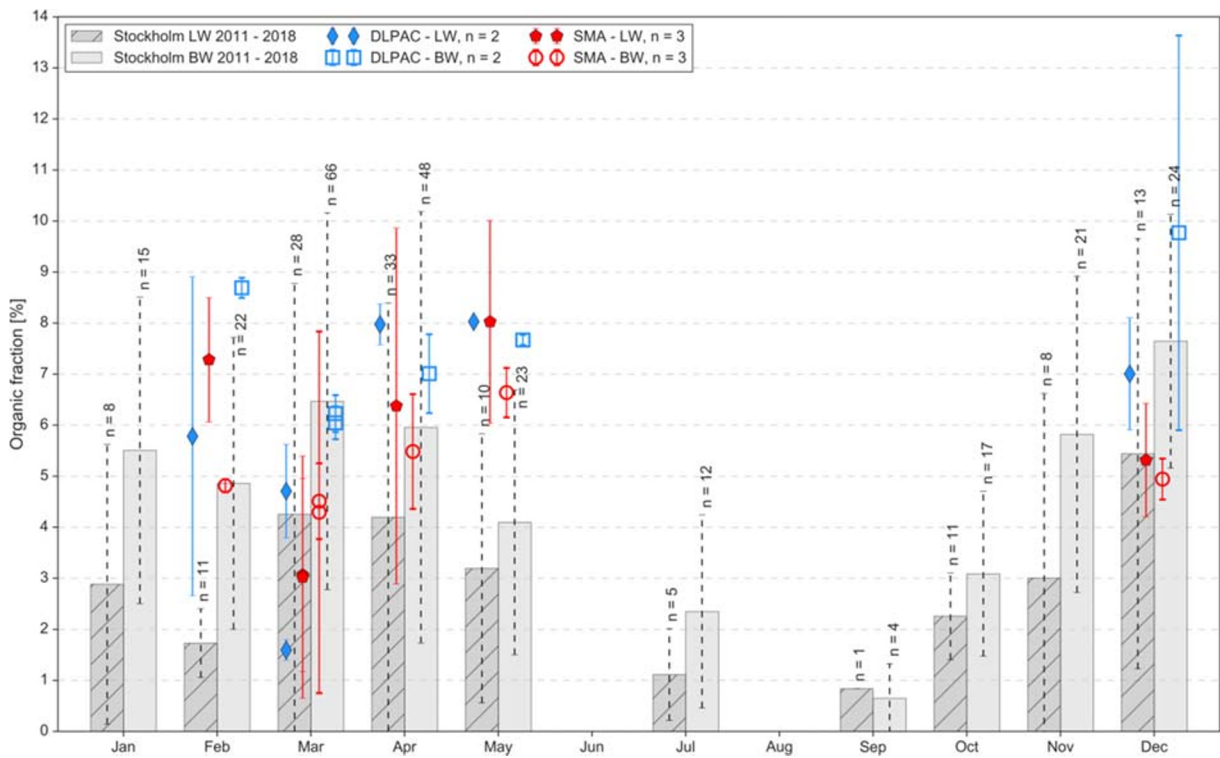
Fig. 8 A comparison of the organic fraction of the dust load from the DLPAC and SMA at Industrigatan, Linköping. The bars express the average organic fraction and the error bars express the standard deviation. The measurements from Industrigatan show the mean value and standard deviation for measurements in that month. The letter *n* marks number of observations. LW, left wheel track; BW, between wheel tracks. In February, two measurements took place at DLPAC and SMA at Industrigatan. Available measurement data from Stockholm (Gustafsson et al. 2014; Gustafsson et al. 2015; Gustafsson et al. 2016; Gustafsson et al. 2017; Gustafsson et al. 2018; Gustafsson et al. 2019a) has been added to the figure for comparison

it is speculated that the dust load available for suspension into air can increase over time before reaching a steady state. However, this long-term variation of the clogging effect on the dust load, a possible steady state, and in continuation air quality, is unknown, thus requiring more in-depth research.

Finally, the investigated SMA was several years older than the DLPAC which may have affected the dust loads observed. On dense pavements, it is known that the abrasion wear from studded tyres is highest during the first year due to the wear of excessive bitumen, aggregates and filler mineral dust residuals from the construction of the pavement (Lundberg et al. 2019b). Thus, the DLPAC is likely to produce more abrasion wear dust during this first season than it will in coming seasons, while simultaneously also having less surface the tyre can interact with which could counteract the increased abrasion wear. For the edge at the SMA specifically, it is possible that the dust load was affected by dust accumulated over

several winter seasons since the road was not regularly cleaned.

3.2 Variation Between Pavement Types and Temporal Variation of the Organic Fraction

The organic fraction of the road dust in the left wheel track and between wheel tracks is presented in Fig. 8 and is compared to similar WDS samplings on dense pavements reported by Gustafsson et al. (2019b) in Stockholm, Sweden. The dust load contained primarily minerals in both Linköping and Stockholm. The organic fraction of the road dust increased during the autumn due to defoliation and then decreased again during winter, where fewer sources were available. During spring, the organic fraction increased due to pollen and vegetation and then decreased until summer, with the expected reduction in pollen. Another aspect was the use of studded tyres during winter, relatively increasing mineral dust from abrasion wear affecting the fractions.
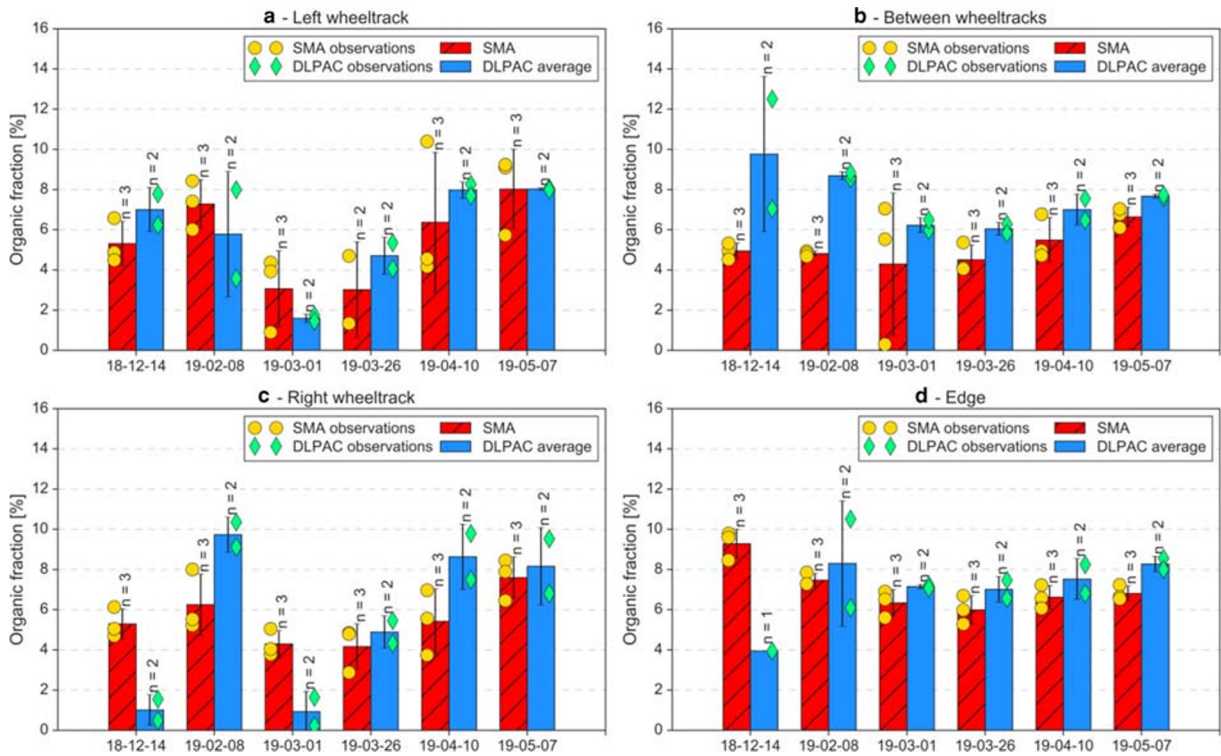
Fig. 9 The variation of the organic fraction of the dust load for the categories left wheel track (**a**), between wheel tracks (**b**), right wheel track (**c**) and the edge (**d**) for the DLPAC and the SMA. The error bars express the standard deviation. The letter n marks the number of observations

Another organic source was the abrasion wear of bitumen during primarily winter, and the year around wear of tyres which depends on the road surface macrotexture and the rubber properties. Bitumen is classified as organic matter due to the method used to separate mineral and organic content. The organic fraction was generally higher for Linköping compared to Stockholm for both categories and did not seem to follow the same pattern over time. The differences were likely primarily due to the difference in availability of organic material and the frequent street cleaning in Stockholm, but also differences in the traffic patterns.

The temporal variation of the organic fraction in the DL_{180} for Linköping is presented in Fig. 9. Mineral dust dominated all samples from both pavements for all categories. Generally, the same cycle as for mineral dust applied. The DLPAC had, in general, a higher organic fraction. Some exceptions were seen in the wheel tracks, and at the edge. Regarding sources, both sites are next to forest areas or grassy areas giving a close local source during autumn and spring, with the DLPAC having slightly more forest vegetation. Abrasion wear of tyres

and bitumen was another possible source. However, it is unknown how much this abrasion wear differentiates between the two pavement types. Since the DLPAC is new, initially, the abrasion wear will increase and thus have a higher contribution of bitumen, although the level is unknown.

3.3 Temporal Variation of the Total Road Dust Load Size Distributions

All size distributions of road dust collected from the SMA had the mode value at particle sizes between 10 and 50 μm (Fig. 10). All measurements showed simple shapes, with a clear tail for finer particle fractions. In some cases, mainly during spring, a hump was visible for coarser particle sizes, implying that the shape consisted of a mixture model influence of at least two size distributions. For both left and right wheel tracks, the highest dust load occurred in winter and diminished during spring, but this was mainly related to the total amount of road dust on the road and not to differences in the size distributions. A larger impact from heavy traffic
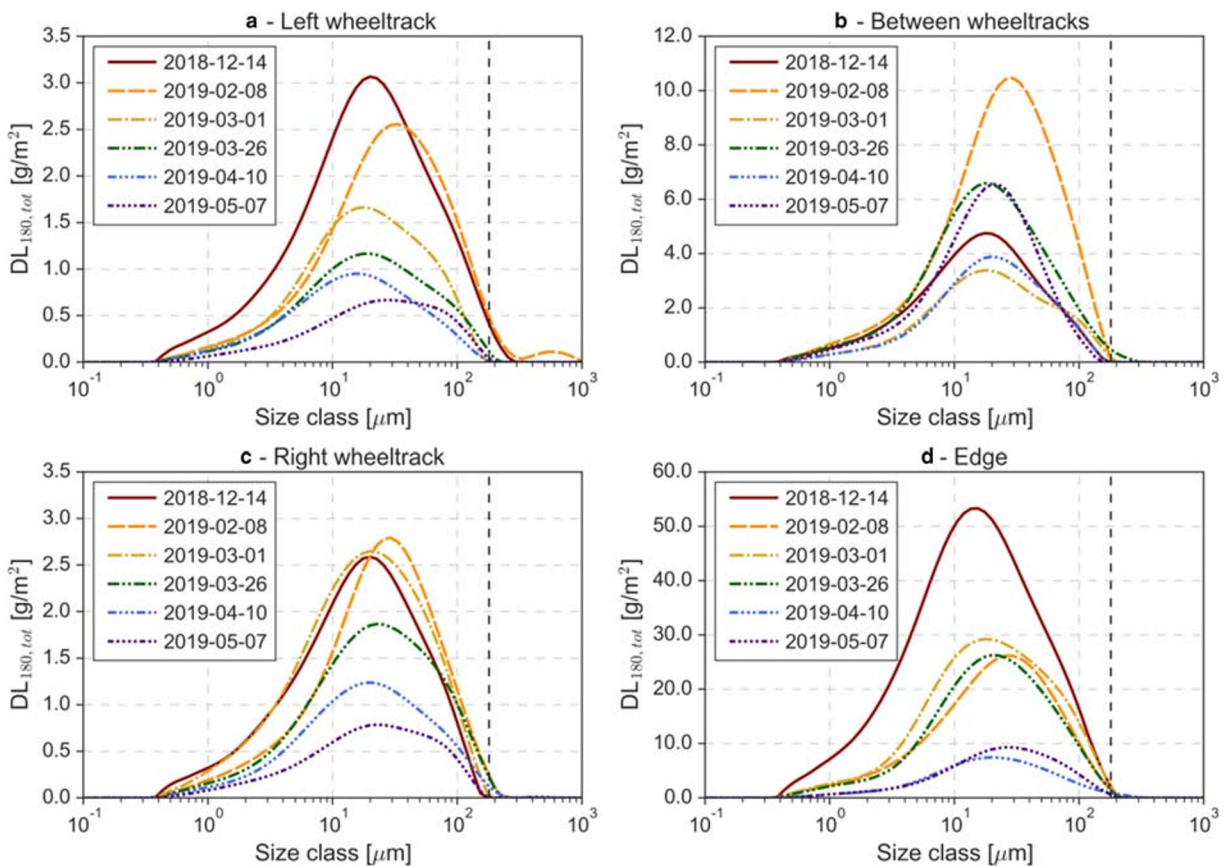
Fig. 10 The absolute size distribution from samples at the SMA for the categories left wheel track (**a**), between wheel tracks (**b**), right wheel track (**c**) and the edge (**d**). The dashed line shows the 180-μm sieve limit

in the right wheel track might explain more humps around 100 μm sizes in the right wheel track compared to the left one. The different levels for all categories can be explained by the variation in dust load and transport processes previously discussed. During late spring, the dust seemingly contained more coarse fractions, implied by the shapes. Finer particles were more easily suspended from the road surface macrotexture than coarser fractions.

All size distributions of road dust collected from the DLPAC had mode values between 10 and 100 μm (Fig. 11). The distributions showed primarily shapes with properties of a mixture model, compared to the shapes of the SMA, with the primary mode around 10–20 μm and the secondary mode around 70–100 μm. The DLPAC also showed slightly larger tails for finer particle fractions than did the SMA. The mode of the particle size seemed to be relatively stable during winter and spring, with some variations. The sample taken in 2019-02-08 in the right wheel track deviated from the other distributions, showing similarity to the SMA distribution. This sample was possibly taken slightly outside the wheel track closer to the edge and at a denser part of the DLPAC. Both left and right wheel tracks showed clearer shapes with the properties of a mixture model than showed between wheel tracks and at the edge. This implies that either the tyres' interaction with the surface or the pavements high interconnected voids or a combination of both influenced the transport of the finest particles and particles between 10 and 100 μm. The DLPAC was possibly more efficient at trapping these types of particles in the air voids compared to the surface macrotexture for dense pavements such as the SMA. Also, the change of the surface with which the tyres interact can possibly limit the generation and suspension of certain particles. As for the SMA, the differences between wheel tracks at the DLPAC could possibly be explained by the difference of tyre passages from the light and heavy vehicles. The right wheel track showed the clearest shapes with properties of a mixture model.
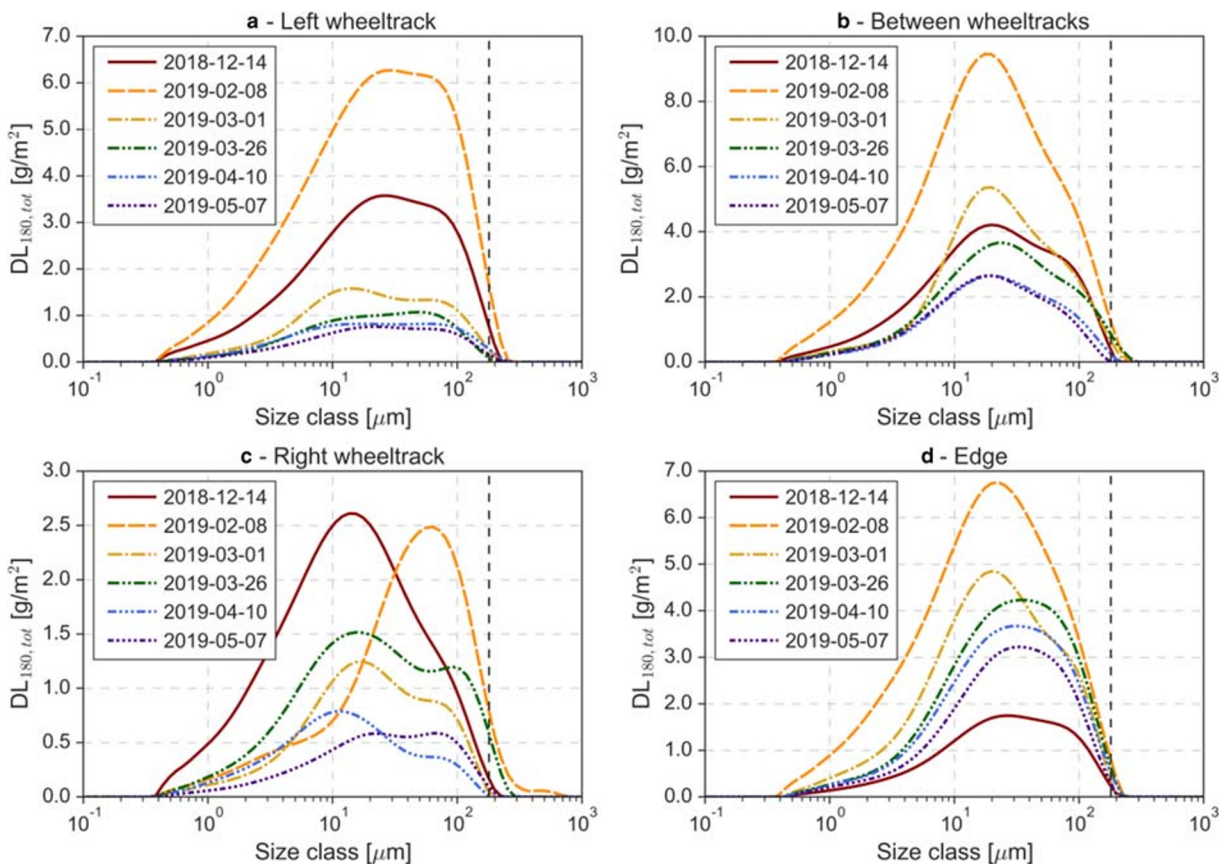
Fig. 11 The absolute size distribution from samples at the DLPAC for the categories left wheel track (**a**), between wheel tracks (**b**), right wheel track (**c**) and the edge (**d**). The dashed line shows the 180-μm sieve limit

Measurements between wheel tracks showed shapes that are in between the shapes of the wheel tracks and the edge. The main difference was the lack of direct interaction with the tyres. The higher turbulent wind flow beneath the vehicle seems to have been less efficient at removing coarser particles. The edge was also affected by turbulence, although diminishing with distance from the traffic and thus reducing the efficiency and further reducing the transport of coarser particles.

The relative size distributions of the road dust are presented in Fig. 12 for the SMA and in Fig. 13 for the DLPAC. This allows a better comparison between the size distributions at different times and at different locations. The DLPAC size distributions had more shapes of a mixture model than their SMA counterparts. Right and left wheel tracks were most similar with flatter modes compared to measurements between wheel tracks and the edge for the DLPAC. A similar pattern was visible for the SMA, although not

as clearly as the DLPAC. As for the absolute size distributions, it seems that the direct interaction with tyres was more efficient at removing particles between 10 and 80 μm at the SMA and between 10 and 100 μm at the DLPAC compared to the transport processes affecting between wheel track and edge, i.e. the lack of direct interaction of tyres. It should also be noted that some of the differences between the pavements could generate different size distributions during abrasion wear. It could also be speculated that the age difference affects the size distribution generated during abrasion wear, although likely only having a minor impact compared to that of the tyre interaction and interconnected air voids.

Finally, Fig. 14 shows the average size distributions for the DLPAC and SMA for each category, with clear differences in both wheel tracks. This difference was due to the change of tyre interaction with the surface and the interconnected voids of the
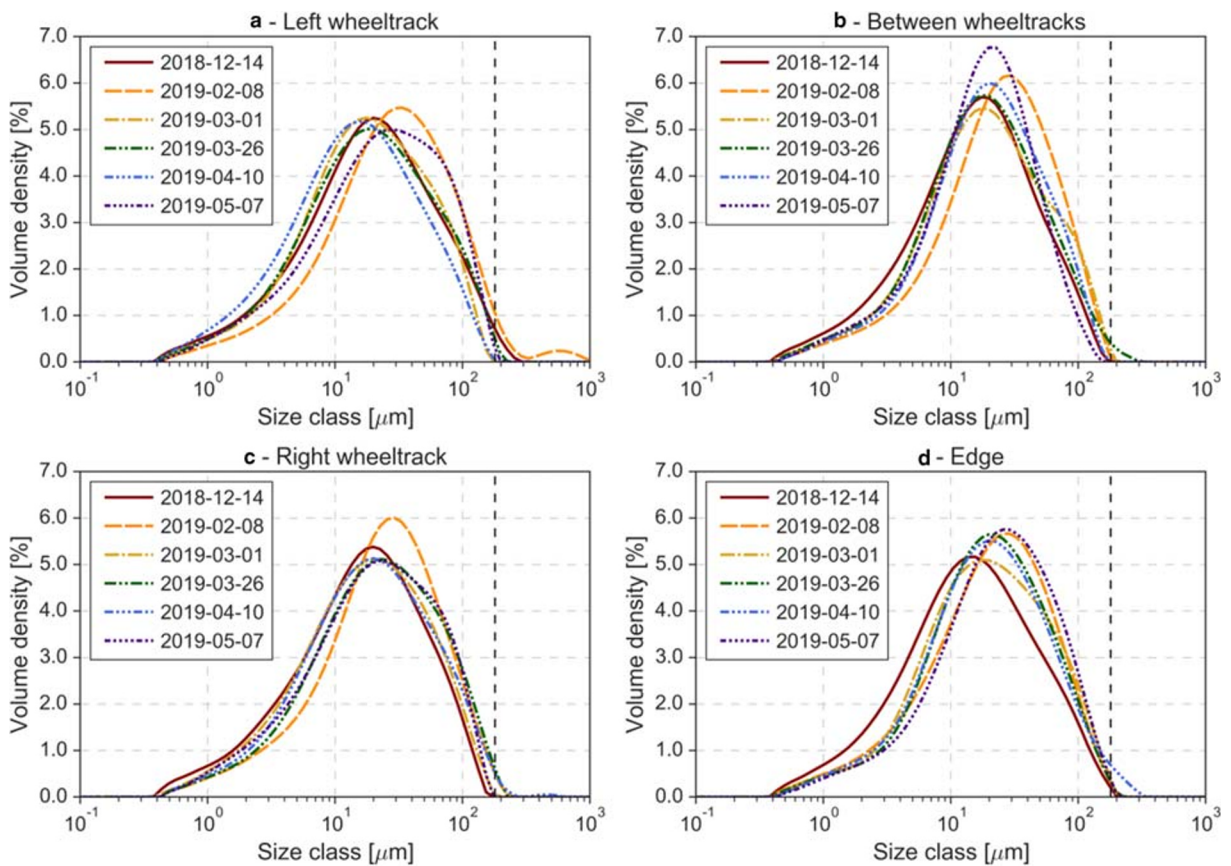
Fig. 12 The relative size distribution from samples at the SMA for the categories left wheel track (**a**), between wheel tracks (**b**), right wheel track (**c**) and the edge (**d**). The dashed line shows the 180-μm sieve limit

DLPAC affecting dust transport and storage. Measurements between wheel tracks and at the edge showed less differences, although there was a hump at coarse fractions for the DLPAC, whilst the SMA had a higher mode.

3.4 Potential Impact of Method Choice on Results and Analysis

The validity of the assumption of representative samples from WDS sampling can be discussed, since Lundberg et al. (2019a) suggest a variable concentration over the sampling time compared to the assumption of a constant concentration. More particles are possibly collected during the beginning compared to the end of a shot. The calculated dust load could be greater than reported, since water retained on the surface has a lower concentration of particles, at least for dense pavements. This caused the presented results to be considered as a lower level of dust load.

Since the assumptions are used for other studies using WDS sampling, this reasoning should hold true for older data, allowing comparisons. The effect is likely small, however, since the average loss of water on a dense pavement is 7–10% of the flushed mass.

Given that porous pavements' primary function is to drain water away from the surface to achieve sufficient friction during wet conditions, it is remarkable that WDS sampling was possible. The likeliest explanation is that the DLPAC bottom layer, which does not conform with the design, thus having lower void content, limited the water drainage speed. This allows sampling of at least some of the water flushed from the WDS. In a DLPAC with a correct bottom layer with higher air void content according to design, dust load available for suspension would be lower due to more effective transport from the top to the bottom layer. Over time, the bottom layer clogs and likely gives the current densification. It is possible that single-layer porous asphalt concrete (SLPAC) could
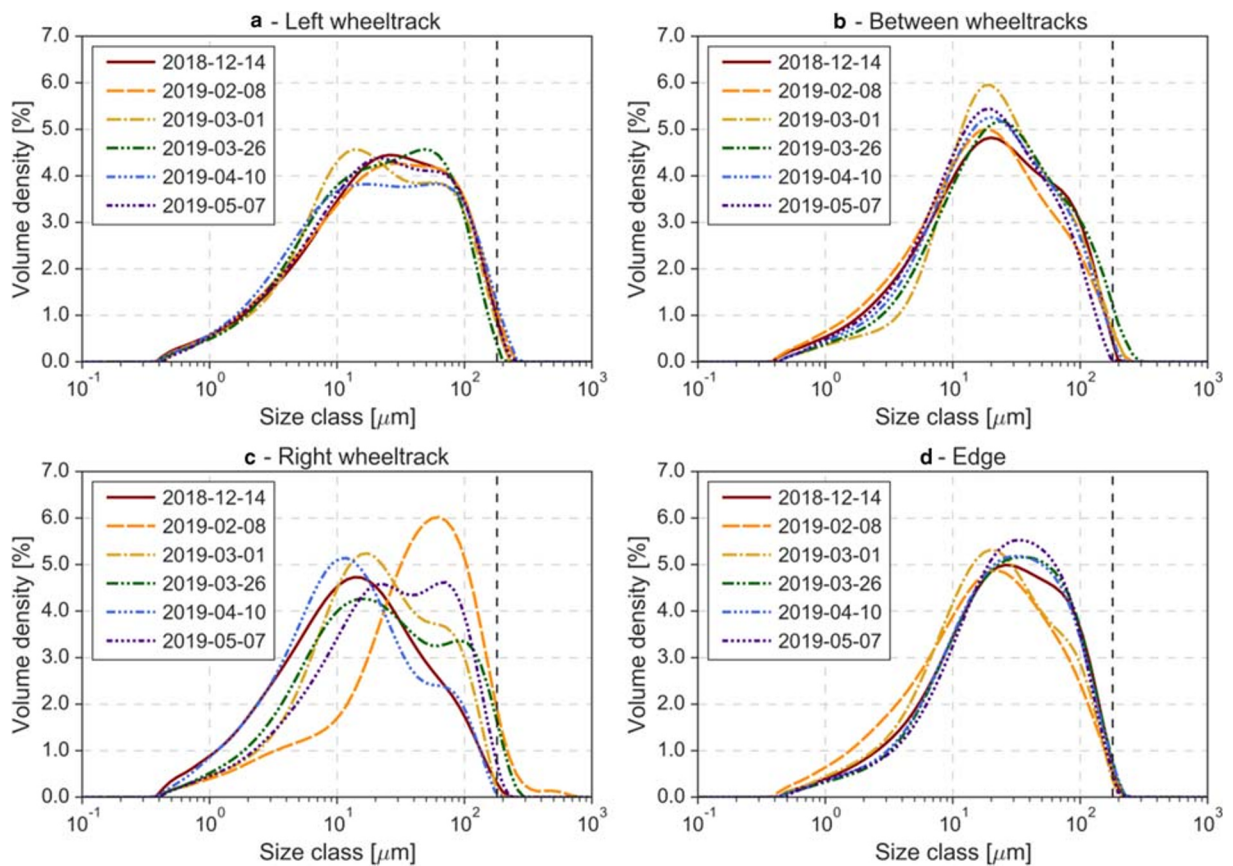
Fig. 13 The relative size distribution from samples at the DLPAC for the categories left wheel track (**a**), between wheel tracks (**b**), right wheel track (**c**) and the edge (**d**). The dashed line shows the 180-μm sieve limit

perform the same as the results presented in this study. Another aspect of WDS sampling on a porous pavement is that the flushed water likely transports particles deeper inside the voids. It is unknown how the size distribution of this flushed dust compares to size distributions of the collected dust. Finer particles are more easily transported with water, while larger and heavier particles are more affected by inertia, causing them to get caught more easily in the complex pattern of interconnected voids. Therefore, some loss of larger fractions was likely.

Sieving of dust at 180-μm diameter sizes to remove the larger particles impacts on the size distributions. The size distribution analysis method has an upper size limit of 2 mm. Given no sieving, the distributions' shapes would have changed, showing less fine material and more coarse materials. Since all samples were treated the same way before determining the size distribution, the results are still comparable.

4 Conclusions

This paper presents the results of the temporal variation of the road dust load, the organic fraction and the absolute and relative size distributions for a porous pavement (the DLPAC) and a dense pavement (the SMA). The measurements cover both winter and spring, two seasons with different meteorological conditions and traffic characteristics (including the use of studded tyres). The results of the lateral distribution of dust for the left wheel track, between wheel tracks, for the right wheel track and at the edge are presented.

The dust load had a clear seasonal variation, where the SMA was comparable to other similar measurements in Stockholm, Sweden, and the dust load was for all samples dominated by minerogenic material. Comparisons between the DLPAC and SMA showed generally similar levels and similar seasonal variation. Some differences were observed between the wheel tracks of the DLPAC. The lateral distribution of dust
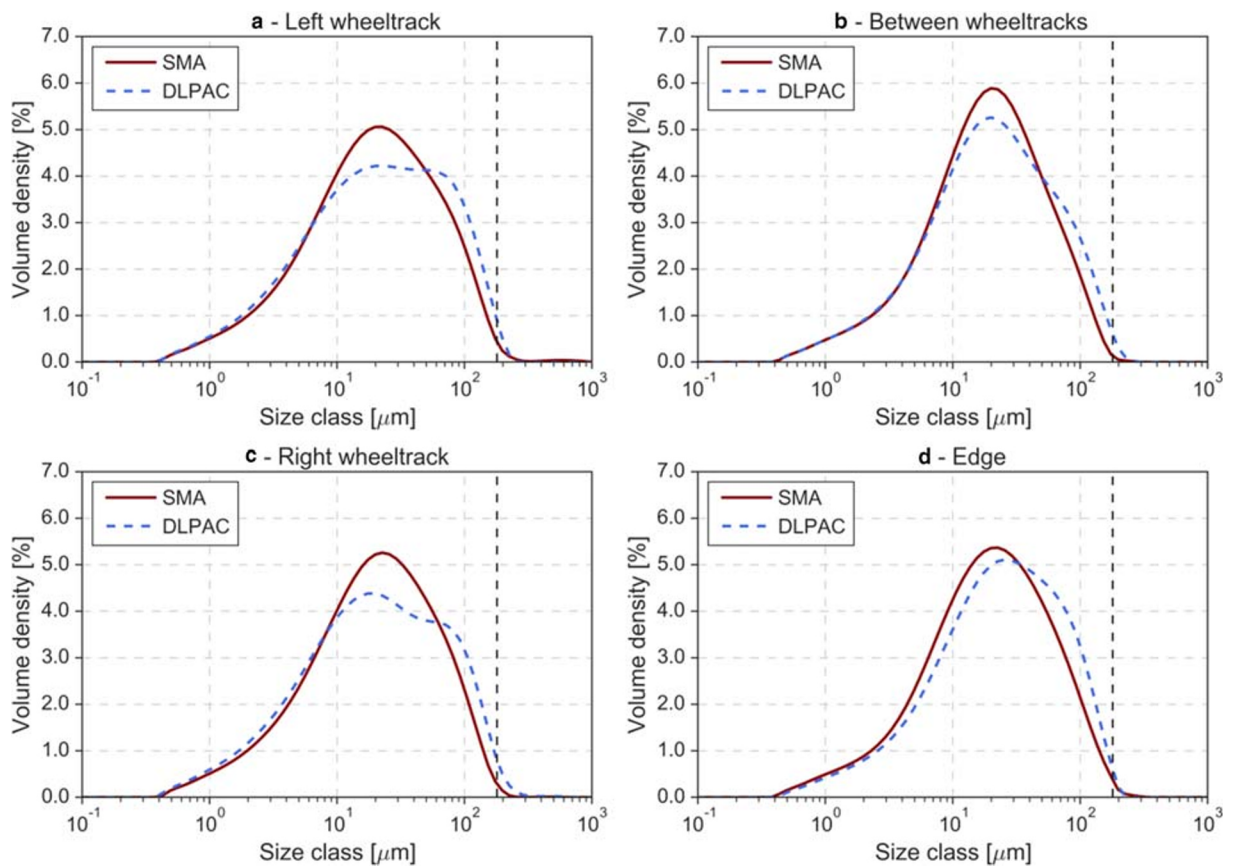
Fig. 14 The average relative size distribution from samples at the SMA and DLPAC for the categories left wheel track (**a**), between wheel tracks (**b**), right wheel track (**c**) and the edge (**d**). The dashed line shows the 180-μm sieve limit

load corresponded with previous sampling from other sites, with lowest loads in the wheel tracks, higher between wheel tracks and highest at the edge.

The DLPAC DL_{180} size distributions showed distinct shapes with properties of a mixture model compared to the shapes of the SMA DL_{180} distributions. The differences between the pavements were most clear in the wheel tracks, and less clear between wheel tracks and at the edge. The impact on the road surface tyre interaction seemed to affect particles sizes between 10 and 100 μm compared to the SMA.

The construction of the DLPAC had a denser bottom layer than the intended design, acting closer to a single-layered porous asphalt. The difference between the pavements can thus be considered a minimum. Since WDS sampling was possible for the DLPAC with denser bottom layer, it indicates that WDS sampling could be possible for thinner single-layer porous pavements, although with unknown effects on the dust size distributions. These differences between the procured and

ordered asphalt, and the constructed asphalt surface course on the road also indicated the importance for road owners to check the delivery quality of the wear course, as well as their specifications of functional properties in their procurements.

Despite the limitations previously discussed, the results obtained give valuable insight into how the pavement type can affect road dust load and its inherent sizes, whilst giving an increased understanding of the road surface tyre interaction mechanisms impacting on dust load dynamics, thus contributing to the currently limited knowledge. The new knowledge improves the understanding of the impact of a pavement type commonly used for noise mitigation, on the dust load and its implications for air quality.

4.1 Suggestions for Future Studies

Based on the experiences from the measurement campaign, the following future studies are suggested:

- Further investigate WDS sampling possibilities on more well-constructed porous pavements.
- Further investigate impact of porous pavements on the size distribution compared to dense pavements.
- Further investigate impact of vehicle class on both dust loads and size distribution.
- Further investigate transport mechanisms of dust inside the porous pavement.
- Investigate variation of dust load and size distributions for several winter seasons to check potential impact on clogging and transport dynamics of the dust for a porous pavement.

Authors' Contributions   Not applicable.

Compliance with Ethical Standards

Conflict of Interest   The authors declare that they have no conflict of interest.

Code Availability   Not applicable.

References

Amato, F., Querol, X., Alastuey, A., Pandolfi, M., Moreno, T., Gracia, J., & Rodriguez, P. (2009). Evaluating urban PM10 pollution benefit induced by street cleaning activities. *Atmospheric Environment, 43*, 4472–4480.

Amato, F., Alastuey, A., De La Rosa, J., Castanedo, Y. G., De La Campa, A. M. S., Pandolfi, M., Lozano, A., Gonzalez, J. C., & Querol, X. (2014a). Trends of road dust emissions contributions on ambient air particulate levels at rural, urban and industrial sites in southern Spain. *Atmospheric Chemistry and Physics, 14*, 3533–3544. https://doi.org/10.5194/acp-14-3533-2014.

Amato, F., Cassee, F. R., Denier Van Der Gon, H. A., Gehrig, R., Gustafsson, M., Hafner, W., Harrison, R. M., Jozwicka, M., Kelly, F. J., Moreno, T., Prevot, A. S., Schaap, M., Sunyer, J., & Querol, X. (2014b). Urban air quality: the challenge of traffic non-exhaust emissions. *Journal of Hazardous Materials, 275*, 31–36. https://doi.org/10.1016/j.jhazmat.2014.04.053.

Amato, F., Favez, O., Pandolfi, M., Alastuey, A., Querol, X., Moukhtar, S., Bruge, B., Verlhac, S., & Orza, J. a. G., Bonnaire, N., Le Priol, T., Petit, J. F. & Sciare, J. (2016). Traffic induced particle resuspension in Paris: emission factors and source contributions. *Atmospheric Environment, 129*, 114–124. https://doi.org/10.1016/j.atmosenv.2016.01.022.

Brunekreef, B., & Forsberg, B. (2005). Epidemiological evidence of effects of coarse airborne particles on health. *European Respiratory Journal, 26*, 309–318. https://doi.org/10.1183/09031936.05.00001805.

Burtscher, H. (2005). Physical characterization of particulate emissions from diesel engines: a review. *Journal of Aerosol Science, 36*, 896–932. https://doi.org/10.1016/j.jaerosci.2004.12.001.

Cen. (2012). *EN 12697-1 - EN 12697-1 - Bituminous mixtures - test methods for hot mix asphalt - Part 1: Soluble binder content*. Brussels: European Committee for Standardization (CEN).

Cen. (2018). *EN 12697-8 - EN 12697-8 - Bituminous mixtures - test methods - Part 8: determination of void characteristics of bituminous specimens*. Brussels: European Committee for Standardization (CEN).

China, S., & James, D. E. (2012). Influence of pavement macrotexture on PM10 emissions from paved roads: a

controlled study. *Atmospheric Environment, 63*, 313–326. https://doi.org/10.1016/j.atmosenv.2012.09.018.

Denby, B. R., Sundvor, I., Johansson, C., Pirjola, L., Ketzel, M., Norman, M., Kupiainen, K., Gustafsson, M., Blomqvist, G., & Omstedt, G. (2013). A coupled road dust and surface moisture model to predict non-exhaust road traffic induced particle emissions (NORTRIP). Part 1: Road dust loading and suspension modelling. *Atmospheric Environment, 77*, 283–300. https://doi.org/10.1016/j.atmosenv.2013.04.069.

Eisenblaetter, J., Walsh, S. J., & Krylov, V. V. (2010). Air-related mechanisms of noise generation by solid rubber tyres with cavities. *Applied Acoustics, 71*, 854–860. https://doi.org/10.1016/j.apacoust.2010.05.002.

Elmgren, M. 2018. Trafikomläggning och ny hårdare asfalt på Folkungagatan, Stockholm - Mätningar och beräkningar av NO2 och PM10. SLB 4:2018. Stockholm: SLB-analys. [In Swedish].

Elmgren, M., & Norman, M. (2019). *Inverkan av bullerreducerande asfalt på PM10-halter och emissioner längs E4 - Sammanställning och utvärdering av mätningar från 2015-2019. SLB 35:2019.* Stockholm: SLB-analys [In Swedish].

Erlingsson, S., Said, S. & Mcgarvey, T. 2012. Influence of heavy traffic lateral wander on pavement deterioration. *Proceedings of the 4th European Pavement and Asset Management Conference,* Malmö, Sweden, 5-7 September, CD-ROM.

Etyemezian, V., Nikolich, G., Ahonen, S., Pitchford, M., Sweeney, M., Purcell, R., Gillies, J., & Kuhns, H. (2007). The portable in situ wind erosion laboratory (PI-SWERL): a new method to measure PM10 potential for windblown dust properties and emissions. *Atmospheric Environment, 41*, 3789–3796. https://doi.org/10.1016/j.atmosenv.2007.01.018.

Forsberg, B., Hansson, H. C., Johansson, C., Areskoug, H., Persson, K., & Jarvholm, B. (2005). Comparative health impact assessment of local and regional particulate air pollutants in Scandinavia. *Ambio, 34*, 11–19.

Grigoratos, T., & Martini, G. (2015). Brake wear particle emissions: a review. *Environmental Science and Pollution Research, 22*, 2491–2504. https://doi.org/10.1007/s11356-014-3696-8.

Gustafsson, M., & Johansson, C. (2012). *Road pavements and PM10. Summary of the results of research funded by the Swedish transport Administration on how the properties of road pavements influence emissions and the properties of wear particles. Report 2012:241.* Borlänge: Trafikverket.

Gustafsson, M., Blomqvist, G., Gudmundsson, A., Dahl, A., Swietlicki, E., Bohgard, M., Lindbom, J., & Ljungman, A. (2008). Properties and toxicological effects of particles from the interaction between tyres, road pavement and winter traction material. *Science of the Total Environment, 393*, 226–240. https://doi.org/10.1016/j.scitotenv.2007.12.030.

Gustafsson, M., Blomqvist, G., Gudmundsson, A., Dahl, A., Jonsson, P., & Swietlicki, E. (2009). Factors influencing PM10 emissions from road pavement wear. *Atmospheric Environment, 43*, 4699–4702. https://doi.org/10.1016/j.atmosenv.2008.04.028.

Gustafsson, M., Blomqvist, G., & Jonsson, P. (2011). *Damningsminimerad vinter- och barmarksdrift. Mått, medel och strategier, VTI Rapport 701.* Linköping: Väg- och transportforskningsinstitutet [In Swedish].

Gustafsson, M., Blomqvist, G., Janhäll, S., Johansson, C., & Norman, M. (2014). *Driftåtgärder mot PM10 i Stockholm : utvärdering av vintersäsongen 2012–2013.* Linköping: VTI [In Swedish].

Gustafsson, M., Blomqvist, G., Janhäll, S., Johansson, C., & Norman, M. (2015). *Driftåtgärder mot PM10 i Stockholm : utvärdering av vintersäsongen 2013–2014.* Linköping: Statens väg- och transportforskningsinstitut [In Swedish].

Gustafsson, M., Blomqvist, G., Janhäll, S., Norman, M., & Johansson, C. (2016). *Driftåtgärder mot PM10 i Stockholm : utvärdering av vintersäsongen 2014–2015.* Linköping: Statens väg- och transportforskningsinstitut [In Swedish].

Gustafsson, M., Blomqvist, G., Janhäll, S., Johansson, C., Järlskog, I., Lundberg, J., Norman, M., & Silvergren, S. (2017). *Driftåtgärder mot PM10 i Stockholm : utvärdering av vintersäsongen 2015–2016. VTI rapport.* Linköping: Statens väg- och transportforskningsinstitut [In Swedish].

Gustafsson, M., Blomqvist, G., Elmgren, M., Janhäll, S., Johansson, C., Järlskog, I., Lundberg, J., Norman, M., & Silvergren, S. (2018). *Driftåtgärder mot PM10 i Stockholm : utvärdering av vintersäsongen 2016–2017. VTI rapport.* Linköping: Statens väg- och transportforskningsinstitut [In Swedish].

Gustafsson, M., Blomqvist, G., Elmgren, M., Johansson, C., Järlskog, I., Lundberg, J., Norman, M., & Silvergren, S. (2019a). *Driftåtgärder mot PM10 i Stockholm : utvärder av vintersäsongen 2017–2018. VTI rapport.* Linköping: Statens väg- och transportforskningsinstitut [In Swedish].

Gustafsson, M., Blomqvist, G., Järlskog, I., Lundberg, J., Janhäll, S., Elmgren, M., Johansson, C., Norman, M., & Silvergren, S. (2019b). Road dust load dynamics and influencing factors for six winter seasons in Stockholm, Sweden. *Atmospheric Environment: X, 2*, 100014. https://doi.org/10.1016/j.aeaoa.2019.100014.

Harrison, R. M., Jones, A. M., Gietl, J., Yin, J., & Green, D. C. (2012). Estimation of the contributions of brake dust, tire wear, and resuspension to nonexhaust traffic particles derived from atmospheric measurements. *Environmental Science and Technology, 46*, 6523–6529. https://doi.org/10.1021/es300894r.

Hussein, T., Johansson, C., Karlsson, H., & Hansson, H. C. (2008). Factors affecting non-tailpipe aerosol particle emissions from paved roads: on-road measurements in Stockholm, Sweden. *Atmospheric Environment, 42*, 688–702. https://doi.org/10.1016/j.atmosenv.2007.09.064.

Jonsson, P., Blomqvist, G. & Gustafsson, M. (2008). Wet dust sampler: technological innovation for sampling particles and salt on road surface. *Seventh International Symposium on Snow Removal and Ice Control Technology, Transportation Research Circular,* E-C126**,** pp. 102-111.

Kampa, M., & Castanas, E. (2008). Human health effects of air pollution. *Environmental Pollution, 151*, 362–367. https://doi.org/10.1016/j.envpol.2007.06.012.

Kupiainen, K. (2007). *Road dust from pavement wear and traction sanding.* Helsinki: University of Helsinki.

Kupiainen, K. J., & Pirjola, L. (2011). Vehicle non-exhaust emissions from the tyre–road interface – effect of stud properties, traction sanding and resuspension. *Atmospheric Environment, 45*, 4141–4146. https://doi.org/10.1016/j.atmosenv.2011.05.027.

Kupiainen, K., Ritola, R., Stojiljkovic, A., Pirjola, L., Malinen, A., & Niemi, J. (2016). Contribution of mineral dust sources to street side ambient and suspension PM10 samples.

Atmospheric Environment, 147, 178–189. https://doi.org/10.1016/j.atmosenv.2016.09.059.

Lundberg, J., Blomqvist, G., Gustafsson, M., & Janhäll, S. (2017). *Texture influence on road dust load*. Zürich: Transport and Air Pollution.

Lundberg, J., Blomqvist, G., Gustafsson, M., Janhäll, S., & Järlskog, I. (2019a). Wet dust sampler—a sampling method for road dust quantification and analyses. *Water, Air, & Soil Pollution, 230*, 180. https://doi.org/10.1007/s11270-019-4226-6.

Lundberg, J., Janhall, S., Gustafsson, M., & Erlingsson, S. (2019b). Calibration of the Swedish studded tyre abrasion wear prediction model with implication for the NORTRIP road dust emission model. *International Journal of Pavement Engineering*, 1–15. https://doi.org/10.1080/10298436.2019.1614585.

Lundberg, J., Vieira, T., Blomqvist, G., Gustafsson, M., Janhäll, S., Genell, A. & Erlingsson, S. (2019c). Influence of a porous pavement on PM10 and noise emissions - initial results. *Poster presentation. European Aerosol Conference (EAC).* Gothenburg, Sweden.

Mcgarvey, T. (2016). *Vehicle lateral position depending on road type and lane width : vehicle position surveys carried out on the Swedish road network. VTI report 892A.* Linköping: Statens väg- och transportforskningsinstitut.

Meister, K., Johansson, C., & Forsberg, B. (2012). Estimated short-term effects of coarse particles on daily mortality in Stockholm, Sweden. *Environmental Health Perspectives, 120*, 431–436. https://doi.org/10.1289/ehp.1103995.

Norman, M., & Johansson, C. (2017). *Emission of PM10 and coarse particles from "silent" asphalt*. Zürich: Transport and Air Pollution.

Norman, M., Sundvor, I., Denby, B. R., Johansson, C., Gustafsson, M., Blomqvist, G., & Janhall, S. (2016). Modelling road dust emission abatement measures using the NORTRIP model: vehicle speed and studded tyre reduction. *Atmospheric Environment, 134*, 96–108. https://doi.org/10.1016/j.atmosenv.2016.03.035.

Padoan, E., Ajmone-Marsan, F., Querol, X., & Amato, F. (2018). An empirical model to predict road dust emissions based on pavement and traffic characteristics. *Environmental Pollution, 237*, 713–720. https://doi.org/10.1016/j.envpol.2017.10.115.

Piarc. (1987). *XVIIIth World Road Congress. Surface Characteristics. Technical Committee Report no. 1.* Brussels: Permanent International Association of Road Congress (PIARC).

Sandberg, U., & Ejsmont, J. A. (2002). *Tyre/road noise reference book*. INFORMEX Esjmont & Sandberg Handelsbolag: Kisa.

Sandberg, U., Mioduszewski, P., & Vieira, T. (2018). *Acoustic lifecycle study if the double-layered porous asphalt on E4 in Huskvarna, Sweden*. Chicago: Inter-Noise 2018.

Sigsgaard, T., Forsberg, B., Annesi-Maesano, I., Blomberg, A., Bolling, A., Boman, C., Bonlokke, J., Brauer, M., Bruce, N., Heroux, M. E., Hirvonen, M. R., Kelly, F., Kunzli, N., Lundback, B., Moshammer, H., Noonan, C., Pagels, J., Sallsten, G., Sculier, J. P., & Brunekreef, B. (2015). Health impacts of anthropogenic biomass burning in the developed world. *European Respiratory Journal, 46*, 1577–1588. https://doi.org/10.1183/13993003.01865-2014.

Stafoggia, M., Samoli, E., Alessandrini, E., Cadum, E., Ostro, B., Berti, G., Faustini, A., Jacquemin, B., Linares, C., Pascal, M., Randi, G., Ranzi, A., Stivanello, E., Forastiere, F., & Group,

M.-P. S. (2013). Short-term associations between fine and coarse particulate matter and hospitalizations in Southern Europe: results from the MED-PARTICLES project. *Environmental Health Perspectives, 121*, 1026–1033. https://doi.org/10.1289/ehp.1206151.

Stojiljkovic, A., Kauhaniemi, M., Kukkonen, J., Kupiainen, K., Karppinen, A., Denby, B. R., Kousa, A., Niemi, J. V., & Ketzel, M. (2019). The impact of measures to reduce ambient air PM10 concentrations originating from road dust, evaluated for a street canyon in Helsinki. *Atmospheric Chemistry and Physics, 19*, 11199–11212. https://doi.org/10.5194/acp-19-11199-2019.

Swedish Transport Administration 2011. TRVKB 10 Bitumenbundna lager, TRV 2011:082, TDOK 2011:266. Borlänge: Swedish Transport Administration. [In Swedish].

Thorpe, A., & Harrison, R. M. (2008). Sources and properties of non-exhaust particulate matter from road traffic: a review. *Science of the Total Environment, 400*, 270–282. https://doi.org/10.1016/j.scitotenv.2008.06.007.

Timmers, V. R. J. H., & Achten, P. a. J. (2016). Non-exhaust PM emissions from electric vehicles. *Atmospheric Environment, 134*, 10–17. https://doi.org/10.1016/j.atmosenv.2016.03.017.

Van Der Gon, H. A., Gerlofs-Nijland, M. E., Gehrig, R., Gustafsson, M., Janssen, N., Harrison, R. M., Hulskotte, J., Johansson, C., Jozwicka, M., Keuken, M., Krijgsheld, K., Ntziachristos, L., Riediker, M., & Cassee, F. R. (2013). The policy relevance of wear emissions from road transport, now and in the future–an international workshop report and consensus statement. *Journal of Air and Waste Management Association, 63*, 136–149. https://doi.org/10.1080/10962247.2012.741055.

Vieira, T. (2018). *Tyre-road interaction: a holistic approach to noise and rolling resistance*. Stockholm: Licentiate of engineering, Kungliga Tekniska högskolan.

Vieira, T., Lundberg, J., Genell, A., Sandberg, U., Blomqvist, G., Gustafsson, M., Janhäll, S. & Erlingsson, S. 2019. Porous pavement for reduced tyre/road noise and improved air quality - initial results from a case study. *26th International Congress on Sound & Vibration.* Montreal.

WHO. (2005). Health effects of transport-ralated air pollution. In M. Krzyzanowski, B. Kuna-Dibbert, & J. Schneider (Eds.), *ATH name of publication?* World Health Organisation: Copenhagen.

WHO. (2011). *Burden of disease from environmental noise: Quantification of healthy life years lost in Europe*. Copenhagen: World Health Organization.

WHO. (2013). *Review of evidence on health aspects of air pollution – REVIHAAP project: final technical report*. Copenhagen: World Health Organization.

WHO. (2016). *Ambient air pollution: a global assessment of exposure and burden of disease*. Geneva: World Health Organization.

WHO Regional Office for Europe Oecd. (2015). *Economic cost of the health impact of air pollution in Europe: clean air, health and wealth*. Copenhagen: WHO Regional Office for Europe.